

# A practical identifiability criterion leveraging weak-form parameter estimation

Nora Heitzman-Breen<sup>1\*</sup>, Vanja Dukic<sup>1</sup> and David M. Bortz<sup>1</sup>

<sup>1</sup>Department of Applied Mathematics, University of Colorado, Boulder, CO, 80309-0526, USA.

\*Corresponding author(s). E-mail(s): [nora.heitzman-breen@colorado.edu](mailto:nora.heitzman-breen@colorado.edu);  
Contributing authors: [vanja.dukic@colorado.edu](mailto:vanja.dukic@colorado.edu);  
[david.bortz@colorado.edu](mailto:david.bortz@colorado.edu);

## Abstract

In this work, we define a practical identifiability criterion,  $(\mathbf{e}, \mathbf{q})$ -identifiability, based on a parameter  $\mathbf{e}$ , reflecting the noise in observed variables, and a parameter  $\mathbf{q}$ , reflecting the mean-square error of the parameter estimator. This criterion is better able to encompass changes in the quality of the parameter estimate due to increased noise in the data (compared to existing criteria based solely on average relative errors). Furthermore, we leverage a weak-form equation error-based method of parameter estimation for systems with unobserved variables to assess practical identifiability far more quickly in comparison to output error-based parameter estimation. We do so by generating weak-form input-output equations using differential algebra techniques, as previously proposed by *Boulier et al* [1], and then applying Weak form Estimation of Nonlinear Dynamics (WENDy) to obtain parameter estimates. This method is computationally efficient and robust to noise, as demonstrated through two classical biological modelling examples.

**Keywords:** Identifiability, Weak form, Data-driven modeling

## 1 Introduction

Parameter estimation is central to mathematical modeling in the biological sciences. However, despite the increasing sophistication of computational techniques over the years, there are many examples of researchers using the same model and obtaining widely varying parameter estimates [2–6]. Therefore, analyzing model identifiability,

i.e., the ability to recover unique parameters of a system from observations, is critical to developing robust and replicable models of biological systems.

*Structural identifiability* addresses whether model parameters can be uniquely determined given the observation of some output variables of a system. There are multiple approaches to assess the structural identifiability of a model including but not limited to a Taylor series expansion [7–9], the implicit function theorem [8, 9], generalizations of observability criteria [10–12], and differential algebra<sup>1</sup> approaches [15–17].

However, in practice, the quantity, frequency, and timing of available data have been shown to have large impacts on the reliability of parameter estimates. For examples in models of acute viral infections, see [2, 18, 19]. Furthermore, choices in the numerical discretizations (needed to approximate solutions) can also impact parameter estimates [20, 21]. *Practical identifiability* refers to whether parameters can be uniquely estimated given the available observations and the chosen parameter estimation method, and is closely related to the uncertainty quantification of model parameters. Some popular techniques to assess practical identifiability involve performing many replicate parameter estimations, which can become computationally expensive depending on the choice of estimation method and the complexity of the model.

Weak-form based parameter estimation, which is typically much faster than output error-based methods, can address the challenge incurred by repeating the parameter estimation. The idea of using the weak form in system identification can be traced back to the Equations-of-Motion method described in [22] in which an equation (in the strong form) is multiplied by a compactly supported test function<sup>2</sup>  $\phi$  and then the equation is integrated. As the derivatives of the test functions are also assumed to have compact support, integration by parts removes the need to evaluate the derivatives of the data. Shinbrot proposed that the  $\phi$ 's be trigonometric functions with different frequencies, while Loeb and Cahen [23] later proposed piecewise polynomials (denoting their approach as the *Modulating Functions Method*). Recently, our group has developed a weak form-based parameter estimation and equation learning method in the spirit of Shinbrot, Loeb and Cahen, but with mathematically motivated test functions [24–26]. This choice of test functions improves both the computational efficiency of performing parameter estimation and is highly robust to noise in the data. These weak form based methods have also been applied to biological and environmental systems [27–29].

One challenge in using this class of direct parameter estimation methods is that all variables must be measured. However, in biological systems, data is rarely observed for all model compartments. For example, epidemiological models are often calibrated to only a subset of model compartments, such as mortality or hospitalization data. Accordingly, researchers have considered differential elimination methods to collapse a system of low-order equations to an equivalent lower-dimensional high-order system with only observable variables [1, 30–32], and in some cases these systems have been cast into either integral or weak forms [1, 32]. However, previous applications of

---

<sup>1</sup>A subfield of algebra created by Ritt and his student Kolchin to study the existence of solutions to differential equations ([13, 14]).

<sup>2</sup>Shinbrot calls them *method functions*

these elimination methods have not yielded a robust weak-form parameter estimation process.

In this work, we propose a process for efficiently assessing *a priori* model identifiability by leveraging weak-form parameter estimation. First, we apply differential elimination methods to generate an input-output equation. At this step, we can also assess the structural identifiability of the model, which is prerequisite to practical identifiability. Second, we cast the input-output equation into its weak-form. Third, we implement a sampling-based method by performing weak-form parameter estimation on simulated data. This method is feasible even for large sample sizes and high levels of measurement error when the Weak form Estimation of Nonlinear Dynamics (WENDy) is used for parameter estimation, due to the method’s robustness to noise and computational efficiency. Finally, we assess practical identifiability from these samples using a newly defined criterion,  $(e, q)$ -identifiability.

In Sections 2.1 and 2.2, we will give a brief overview of input-output-based methods to determine structural identifiability and methods used to determine practical identifiability. Then, in Section 2.3, we define  $(e, q)$ -*identifiability*, a practical identifiability criterion based on the noise in observed variables and the mean-square error for the parameter estimator. Next, in Section 3.1 we describe the generation of weak-form input-output and weak-form parameter estimation. These methods are applied together for two canonical biological examples in Section 3.2. Finally, in Section 4 we apply our definition of  $(e, q)$ -identifiability to the examples, compare this criterion to the average relative error, and lastly compare the computational efficiency of the weak-form parameter estimation to an output error method.

## 2 Background

In Sections 2.1 and 2.2, we provide background information on structural and practical identifiability. Readers already familiar with these topics are encouraged to skip to Section 2.3, in which, we introduce  $(e, q)$ -*identifiability*, a practical identifiability criterion based on relating the noise in observed variables and the mean-square error for the parameter estimator.

### 2.1 Structural Identifiability

The goal of studying the structural identifiability of a system of differential equations is to determine whether there are unique model parameters that give rise to the dynamics of the observable states. This property is a prerequisite to recovering parameters of interest from partially observed systems. Below, we provide a brief overview of the input-output based method of determining structural identifiability, along with some standard definitions.

Consider the system of ordinary differential equations  $\dot{U} = \Theta(U, w)$ , where  $U$  is a vector of the state variables of the system and  $w$  is a vector of model parameters. If the observations (output of the system) are given by  $y(t) = \Omega(U, w)$ , then structural identifiability can be defined as follows.

**Definition 1.** Let  $w$  and  $\hat{w}$  be distinct model parameter vectors. A model is said to be globally structurally identifiable when

$$\Omega(U, w) = \Omega(U, \hat{w}) \Rightarrow w \equiv \hat{w}.$$

A model is said to be locally structurally identifiable if for any  $w$  within an open neighborhood of some point  $\hat{w}$  in the parameter space,

$$\Omega(U, w) = \Omega(U, \hat{w}) \Rightarrow w \equiv \hat{w}.$$

One way of assessing the structural identifiability of a system of differential equations is by studying the input-output equation. Input-output equations have been used to study the structural identifiability of numerous biological systems, for examples, see [19, 33–35]. An input-output equation is a differential equation that depends only on the inputs, outputs, their respective derivatives, and the model parameters. Given an input-output equation for a system of differential equations, global structural identifiability can be restated as given below.

**Definition 2.** A model is said to be globally structurally identifiable if coefficient map of the corresponding input-output equation,  $c(w)$  is injective.<sup>3</sup>

Input-output equations can be found from a system of differential equations using differential elimination algorithms, including the Ritt, the Ritt-Kolchin [14], and the Rosenfeld-Groebner [36] algorithms. There are many computational tools available to obtain input-output equations, including [17, 37, 38]. In this study, we use the `DifferentialAlgebra` v4 package [39] in Python to generate input-output equations, which applies a Rosenfeld-Groebner algorithm.

## 2.2 Practical Identifiability

In practice, observations of the state variable are often sparse and subject to measurement error. Practical identifiability refers to whether parameters can be uniquely estimated given the available observations and chosen estimation method. Below, we provide a brief overview of current methods to determine practical identifiability and propose a criterion for practical identifiability based on the mean-square error observed for the parameter estimator.

There are many proposed methods to assess the practical identifiability of a system, and there is no commonly agreed-upon single criterion to determine practical identifiability. The Fisher Information Matrix (FIM) can be used to approximate the parameter covariance matrix and as a measure of local practical identifiability [40, 41], however, this criterion is not always generalizable to nonlinear systems. The FIM method has been used to assess the practical identifiability in biological systems [3, 33]. Profile Likelihood based methods test practical identifiability through successive refittings in the parameter space, which give insight into the shape of the likelihood and whether it is uniquely maximized [42]. Profile likelihood methods have been used to

---

<sup>3</sup>Local structural identifiability can be similarly restated.

assess practical identifiability in biological systems as well [35, 43]. However, methods, like Profile Likelihood, rely on the special relationship between the output error objective function and the maximum likelihood.

Sampling-based methods of assessing practical identifiability involve repeated estimation performed using a prescribed error model for the observed data. From these repeated estimations, one criterion that has been proposed to assess practical identifiability is the average relative error. Examples of this criterion applied to biological systems include [19, 44]. Sampling-based methods can be applied to any choice of objective function, but they also require numerous repetitions of the chosen parameter estimation method, which can become challenging to implement if the estimation method is not computationally efficient.

### 2.3 (e,q)-identifiability

We are interested in using a sampling-based method of assessing practical identifiability. By choosing such a method, we can avoid making assumptions about the local linearization of the system, which is required to find the Fisher Information Matrix. And, we do not need to restrict our choice of objective function, which is needed for Profile Likelihood Analysis. While sampling-based methods can pose a computational challenge, recent advances in weak-form parameter estimation can be leveraged to perform the many required repetitions of the estimation quickly.

We propose a practical identifiability criterion that depends on the mean-squared error and a fixed level of additive error in the data. Below we define the (e,q)-identifiability, which can be computed for systems and data using either output error or equation error optimization.

First, we define the error structure of the model observations.

**Definition 3.** Let  $y(t)$  be observations of the model  $\dot{U} = \Theta(U, w)$  with some associated measurement noise so that

$$y(t) = \Omega(U, w) + \epsilon,$$

where  $\epsilon \sim \mathcal{F}$  and  $\mathcal{F}$  is an arbitrary distribution with variance  $\sigma^2$ .

Next, we define a scalar that describes the size of the measurement error relative to the size of the data measurements.

**Definition 4.** Let  $e$  denote the additive error ratio such that  $\sigma = eRMS(\Omega(t))$ , where RMS is the root mean square, i.e.,  $RMS(\Omega(t)) = \sqrt{\frac{1}{T} \int_0^T \Omega(t)^2}$ .

Next, we define a scalar that describes the size of the error in parameter estimates relative to the size of the parameter.

**Definition 5.** Let  $q$  denote the estimate error ratio such that  $M_i = (q|w_i|)^2$ , where  $M_i$  is the maximum tolerated value of some error measurement in the parameter estimator,  $\hat{w}_i$ .

Note that in the case that the true parameter value is unknown, we let  $M_i = \mathbb{E}(\hat{w}_{i,k})$ . Finally, we define an identifiability criterion relating these two ratios.

**Definition 6.** A parameter is said to be **(e, q)-identifiable** if, for a given additive error ratio,  $e$ , the mean-squared error (MSE) of the parameter estimator,  $\hat{w}_i$ , is below  $M_i$ , i.e.,

$$MSE(\hat{w}_i(\mathbf{e})) < (q|w_i|)^2 .$$

Furthermore, a model is said to be **(e, q)-identifiable** if the above holds for all  $i$ .

Here,  $MSE(\hat{w}) = \mathbb{E}[(\hat{w}_k - w)^2] = \text{Var}(\hat{w}) + \text{Bias}(\hat{w}, w)^2$ . Since the MSE can be decomposed into the variance and squared bias,  $(e, q)$ -identifiability indicates that we can obtain parameter estimates that are both near the true parameter and near each other with respect to a cut-off,  $(q|w|)^2$ , that is scaled by the size of the parameter and the choice of acceptable estimate error ratio  $q$ .

### 3 Weak-form Input-output equations

In this section, we combine established differential elimination methods with recent advances in weak-form parameter estimation to accurately estimate parameters from systems with unobserved compartments. In Section 3.1, we describe a method to generate weak-form input-output equations by using differential elimination, then briefly present a method of parameter estimation using these equations. Lastly, in Section 3.2, we illustrate the application of these methods to two canonical biological systems.

#### 3.1 Weak-form parameter estimation for systems with unobserved variables

In general, we convert between an equation in the form  $\dot{U} = \Theta(U, W)$ , with observed states,  $y(t) = \Omega(U, W)$ , to an input-output equation of the form  $0 = F(y)$ . This process involves, first, ranking the model variables and their derivatives with the observed state variable at the lowest rank. Next, differential polynomials generated from the model equations are reduced to their characteristic set according to the new ranking using a differential elimination algorithm. After the characteristic set is obtained, the lowest ranking differential polynomial(s) will be the input-output equation(s).

If the right-hand side of the input-output equation can be written in the form

$$F(y) = \sum_{i=0}^n \frac{d^i}{dt^i} H_i(y), \quad (1)$$

then it is clear that by convolving the input-output equation with a test function  $\phi$  and applying integration by parts that we can generate a weak-form input-output equation of the form

$$0 = \sum_{i=0}^n \int_0^T (-1)^i \left( \frac{d^i}{dt^i} \phi(t) \right) H_i(y) dt. \quad (2)$$

However, not all nonlinear systems can be written in the form of equation (1). In the case that the right-hand side of the input-output equation takes the form,

$$F(y) = \sum_{i=0}^n K_i(y) \frac{d^i}{dt^i} H_i(y), \quad (3)$$

either substitutions of variables, estimation of higher order derivatives from data, or both will be required to compute terms that are not integrable by parts.

Recently, our group has developed the Weak form Estimation of Nonlinear Dynamics (WENDy) method for parameter estimation [26]. Briefly, in the WENDy method, a system is cast in its weak form, then data is substituted directly into the equation, and parameters are estimated by solving a regression problem. A more detailed description of the method can be found in [26], and specifics about the implementation of WENDy in this study are given in Appendix A. Most importantly, this allows us to estimate parameters from systems in the form of (2) directly using WENDy.

### 3.2 Illustrating Examples

We present two example systems whose input-output equations take on the forms of equations (1) and (3) when a single state variable is observed.

**Example 3.1.** We are motivated by an example [1] where a weak-form input-output equation is used to estimate parameters in the blood-tissue diffusion model. Diffusion of drug between blood and tissue in the body is assumed to be proportional to the concentration gradient, and is represented by the following equation,

$$\begin{aligned} \dot{x}_1(t) &= -k_{12}x_1(t) + k_{21}x_2(t) - \frac{V_e x_1(t)}{1 + x_1(t)}, \\ \dot{x}_2(t) &= k_{12}x_1(t) - k_{21}x_2(t), \end{aligned} \quad (4)$$

where  $x_1$  and  $x_2$  are the concentrations of drug in the blood and tissue, respectively,  $k_{12}$  is the diffusion rate from the blood into the tissue,  $k_{21}$  is the diffusion rate from the tissue into the blood, and  $V_e$  is the rate of drug decay in the blood. The input-output equation corresponding to (4) when only  $x_1(t)$  is observed, can be written in the form of (1), and the weak-form input-output equation for the blood diffusion model is given below,

$$- \int_{T_1}^{T_2} \ddot{\phi} x_1(t) dt = w_1 \int_{T_1}^{T_2} \phi \frac{x_1(t)}{x_1(t) + 1} dt - w_2 \int_{T_1}^{T_2} \dot{\phi} \frac{x_1(t)^2}{x_1(t) + 1} dt + w_3 \int_{T_1}^{T_2} \dot{\phi} \frac{1}{x_1(t) + 1} dt, \quad (5)$$

where  $w_1 = k_{21}V_e$ ,  $w_2 = k_{12} + k_{21}$ , and  $w_3 = k_{12} + k_{21} + V_e$ .

For this example, we consider three choices for the form of the test function,  $\phi$ . We consider  $C^\infty$  bump functions, which have been used in [26]. These functions are

given by the following form,

$$\phi(t, a) = \begin{cases} C \exp(-\frac{\eta}{1-(t/a)^2}), & [-a, a] \\ 0, & elsewhere, \end{cases} \quad (6)$$

where  $C$  is chosen so that  $\|\phi\|_2 = 1$ ,  $a$  is the radius of support, and  $\eta$  is a shape parameter. For this example,  $a = 6$  and  $\eta = 9$ .

We also consider Hartley modulating functions, which were applied to this weak-form system in [1]. Below we give the equation for a third order Hartley modulating function,

$$\phi(t, a) = \begin{cases} C(\text{cas}(\frac{6\pi}{a}t) - 3\text{cas}(\frac{4\pi}{a}t) + 3\text{cas}(\frac{2\pi}{a}t) - 1), & [-a, a] \\ 0, & elsewhere, \end{cases} \quad (7)$$

where  $C$  is chosen so that  $\|\phi\|_2 = 1$ ,  $a$  is the radius of support, and  $\text{cas}(t) = \cos(t) + \sin(t)$ . For this example,  $a = 8$ .

We also consider polynomial test functions, which were shown to be highly robust to noise in [25]. Below we give the equation for a 12<sup>th</sup> order polynomial test function,

$$\phi(t, a) = \begin{cases} C(t+a)^6(a-t)^6, & [-a, a] \\ 0, & elsewhere, \end{cases} \quad (8)$$

where  $C$  is chosen so that  $\|\phi\|_2 = 1$  and  $a$  is the radius of support. For this example,  $a = 8$ .

Figure 1 shows the drug diffusion system fit to only blood concentration using WENDy with a polynomial test function, and Figure 2 shows the average relative error using WENDy for various additive noise ratios for three different test functions. In comparison to [1], WENDy performs competitively, remaining under 50% relative error with 80% white noise in the observed variable when using a 12<sup>th</sup> degree polynomial test function. This figure clearly demonstrates that the choice of test function greatly impacts the robustness of the parameter estimation method.

**Example 3.2.** The SIR model describes the spread of an infection in a population. Susceptible individuals ( $S$ ) become infected ( $I$ ) at a rate  $\beta$  and recover ( $R$ ) without chance of reinfection at a rate  $\alpha$ . Model equations are presented in the equation below,

$$\begin{aligned} \dot{S} &= -\beta SI, \\ \dot{I} &= \beta SI - \alpha I, \\ \dot{R} &= \alpha I. \end{aligned} \quad (9)$$

We assume the infected compartment is the only state variable observed. We then obtain the SIR input-output equation for the observed state variable  $I$ ,

$$0 = -\frac{\dot{I}^2}{I} + \beta\alpha I^2 + \beta I\dot{I} + \ddot{I}. \quad (10)$$

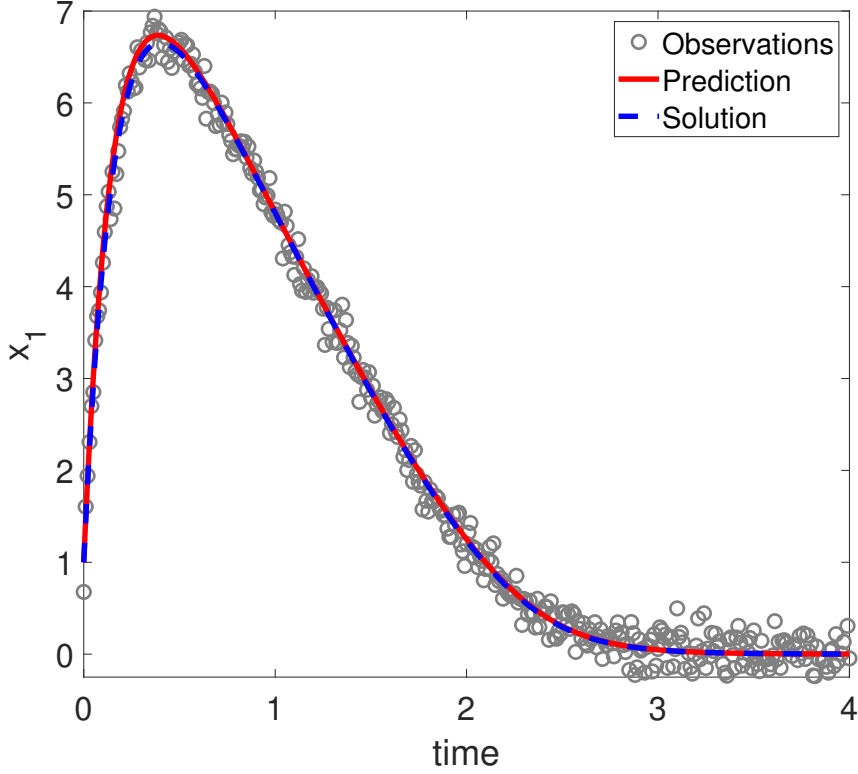


**Fig. 1** Using WENDy with equation (5) we recover parameters for the blood diffusion model (4) with only observations in the blood compartment ( $x_1(t)$ ). The drug concentration dynamics in the blood compartment (red) and the tissue compartment (blue) are given for model (4) with parameters  $k_{12} = 5$ ,  $k_{21} = 1$ , and  $V_e = 6$ . We estimate the true parameters using WENDy from 400 observations of the blood compartment (black dots) with  $e = 5\%$  additive error ratio. Note that  $e = 5\%$  additive error ratio is equivalent to the white noise of  $\sigma = 25.06\%$  for this choice of model parameters.

Note that, as expected, both parameters  $\beta$  and  $\alpha$  of model eq(9) are globally structurally identifiable. From equation (10) we can generate the weak form of model (9), SIR system for observed state  $I$  is presented below,

$$\int_0^T \ddot{\phi} I dt - \int_0^T \dot{\phi} \frac{\dot{I}^2}{I} dt = \beta \int_0^T \dot{\phi} \frac{I^2}{2} dt - \beta \alpha \int_0^T \phi I^2 dt. \quad (11)$$

In this case we are unable to simplify the term  $\int_0^T \dot{\phi} \frac{\dot{I}^2}{I} dt$  using integration by parts. However, let the total population  $N$  be constant,  $N = S(t) + I(t) + R(t)$ , and additionally, re-write  $R$  in terms of only the observed variable  $I$ ,

$$R(t) = \int_0^t \alpha I(s) ds. \quad (12)$$

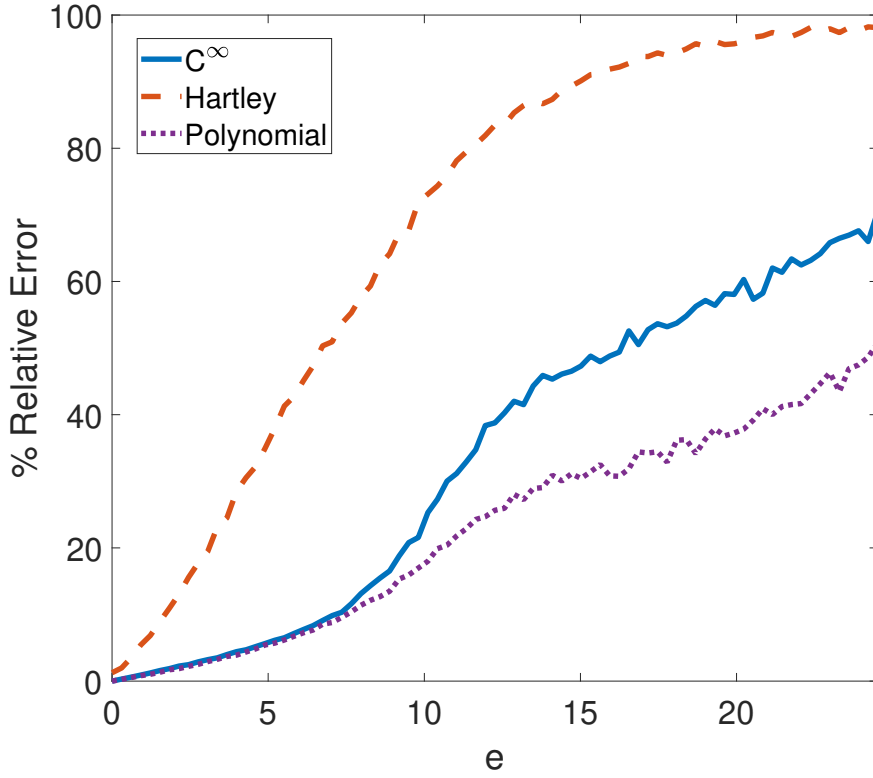


**Fig. 2** Using WENDy with equation (5) is robust to noise. The average relative error for 1,000 simulated data sets with additive Gaussian error ratio  $e \in [0\%, 24.5\%]$  is given for choice of  $C^\infty$  (see Eq. (6)), Hartley (see Eq. (7)), and Polynomial (see Eq. (8)) test functions. This is error ratio is equivalent to additive white noise of the level  $\sigma \in [0, 0.8]$ .

Then, using equations (11)-(12), we define a weak-form SIR model that can be used to estimate the parameter  $\beta$  below,

$$\begin{aligned}
\int_0^T \ddot{\phi} I dt - \alpha^2 \int_0^T \phi I dt &= \beta \int_0^T \dot{\phi} \left( \frac{I^2 - (N - R(t) - I)^2}{2} \right) dt \\
&\quad - \beta \alpha \int_0^T \phi (I^2 + 2(N - R(t) - I)I) dt, \quad (13) \\
R(t) &= \int_0^t \alpha I(s) ds.
\end{aligned}$$

Figure 3A shows the SIR model fit to only the infected population using WENDy.

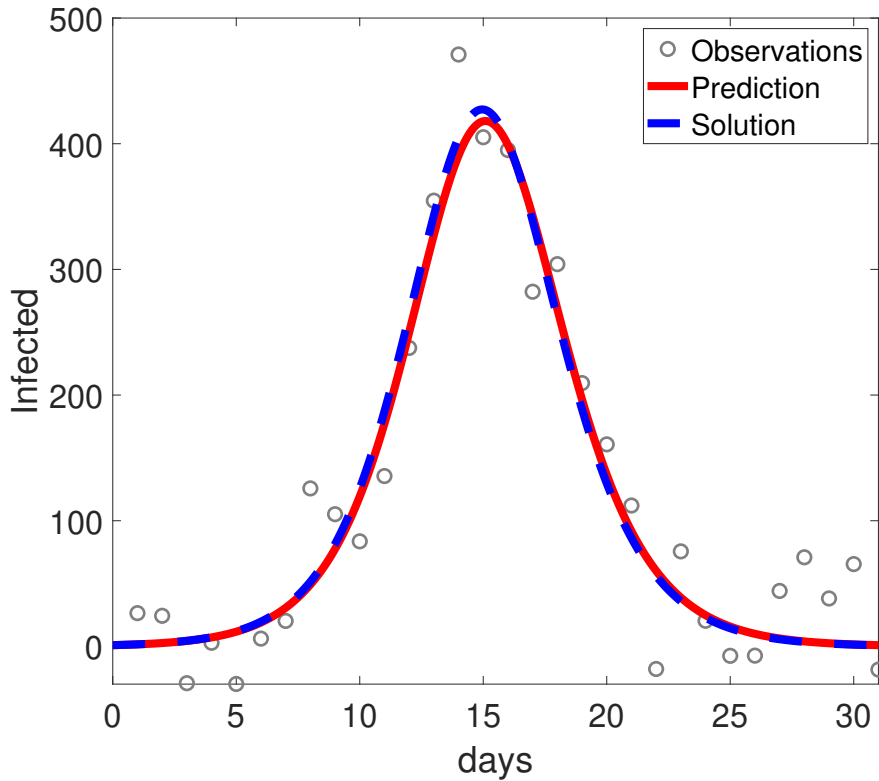


**Fig. 3** Using WENDy with equations (13) we recover the transmission rate  $\beta$  for the SIR model (9) with only observations in the infected compartment, even with large observational noise. The infected compartment dynamics are given for model (9) with  $N=10,000$ ,  $S_0 = N - 1$ ,  $I_0 = 1$ ,  $R_0 = 0$ ,  $\beta = \frac{5.5}{N}$ ,  $\gamma = 5$ . We estimate the true value of  $\beta$  using WENDy from 31 observations of the infected compartment (black dots) and recover the original dynamics (red line) observations with  $e = 20\%$  additive error ratio (Right).

## 4 Examples of Practical Identifiability

In this section, we will describe the Practical identifiability of the weak form systems of the examples generated in Section 3.1. In Section 4.1, we describe the method of generating simulated datasets and parameter estimation. In Section 4.2, we interpret the practical identifiability of two biological examples.

### 4.1 Applying (e,q)-identifiability

To assess the practical identifiability of examples 3.1 and 3.2 we generated simulated data sets of size  $N = 1,000$  for choices of additive noise ratios between  $e = [0\%, 20\%]$  and  $e = [0\%, 80\%]$ , respectively. We generated noisy observations using definition 3 and assuming a Gaussian additive error distribution. For each example, we assumed a

limited number of data points; specifically, 40 observations were considered for Example 3.1, and 31 observations were considered for Example 3.2. Parameter estimates were generated using the WENDy method described in Section 3.1 and Appendix A.

Additionally, we compare the performance of WENDy to a traditional output error (OE) method. We implement the OE method in MATLAB using the function `lsqnonlin` with default settings. To perform the forward solves required by the OE method we use a variable-step, variable-order solver based on the numerical differentiation formulas (NDFs) of orders 1 to 5, as implemented in `ode15s` in Example 3.1 and a Dormand-Prince method as implemented in `ode45` in Example 3.2.

## 4.2 Results of practical identifiability

We estimate the parameters  $w_1$ ,  $w_2$ , and  $w_3$  from the weak-form input-output equation (5) using WENDy (see Appendix A) for simulated data with Gaussian additive error. We vary the measurement additive error ratio in the simulated data between  $e \in [0\%, 20\%]$  such that the standard deviation of the additive error is  $\sigma = e\text{RMS}(\Omega(t))$ , and at each additive error ratio, we generate 1,000 noisy data sets. The  $(e, q)$ -identifiability (see Section 2.2) for  $e \in [0\%, 20\%]$  and  $q \in [1\%, 100\%]$  of model (5) is given in Figure 4A, where the area in blue represents where the model is  $(e, q)$ -identifiable. For example, the model is (5,50)-identifiable, meaning that at a 5% additive error ratio in the data, the MSE of the parameter estimates  $\hat{w} = [\hat{w}_1, \hat{w}_2, \hat{w}_3]$  falls below  $50\% \times w_i$ . However, at 15% measurement additive error ratio, this property no longer holds, i.e., the model is not (15,50)-identifiable. We also observe from the  $(e, q)$ -identifiability of the individual parameters that the identifiability parameter  $w_3$  is lost first as noise increases. In the example above, both  $w_2$  and  $w_3$  are (15, 50)-identifiable, while  $w_1$  is not. As demonstrated in Figure 4A, as additive error increases, the MSE increases and approaches the magnitude of the true parameters.

We additionally compare the  $(e, q)$ -identifiability of model (5) to the average relative error and the coverage of the 95% confidence intervals generated at each additive error ratio. Previous work by our group and others [19, 44] proposed (over many data sets generated at a particular additive error ratio) that a model can be considered practically identifiable in terms of relative error, if the relative error is equal to or lower than the error introduced through additive noise. The relative error generated for 1,000 simulated data sets at each additive error level is given in Figure 4B, and the coverage of the 95% confidence intervals for  $\hat{w}_1$ ,  $\hat{w}_2$ , and  $\hat{w}_3$  are given in Figure 4C. Based on this strict relative error criterion, the blood concentration model is not practically identifiable for any error level. Even at 1% additive noise, the relative error in parameter  $w_3$  is 1.1%. However, a more relaxed condition on relative error for practical identifiability has been used in [19], where relative error needs only to be below  $10e$ . In this case, the blood concentration model is practically identifiable with respect to the relative error from  $e = [0\%, 20\%]$ . Generally, the relative error remains near  $2 \times e$  for parameters  $w_1$  and  $w_2$  and near  $3 \times e$  for parameter  $w_3$  for  $e = [0\%, 20\%]$ . Additionally, above the 11% additive error level, where the model is no longer  $(e, 50)$ -identifiable, the coverage for all parameters  $w_1$ ,  $w_2$ , and  $w_3$  decreases as shown in Figure 4C. For parameters  $w_1$  and  $w_2$  at error levels below  $e = 6\%$  in all trials, the 95% confidence interval contains the true values of  $w_1$  and  $w_2$ . This decreases

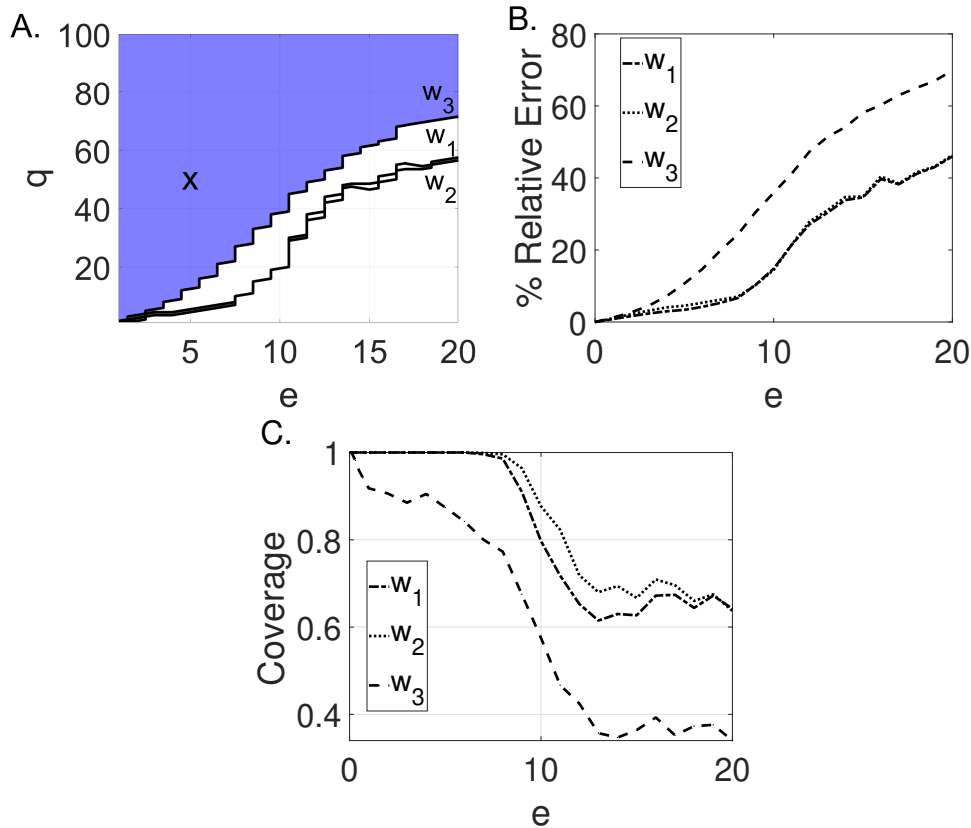


**Fig. 4** Using WENDy with equation (5) we find the blood concentration model to be generally practically identifiable below 11% scaled noise in the data. (A.) The area in blue denotes where the model is  $(e, q)$ -identifiable, and the area in white denotes where the model is not  $(e, q)$ -identifiable. The  $(e, q)$ -identifiability was determined from 1,000 samples at each respective error level,  $e$ . The black **X** denotes the  $(5, 50)$ -identifiability cutoff. Because this point falls within the blue region, we can say that at a 5% additive error ratio in the data the MSE of  $\hat{w}_1$ ,  $\hat{w}_2$ , and  $\hat{w}_3$  remain below the square of 50% the parameter magnitude. (B.) The relative error determined from 1,000 samples at each respective error level,  $e$ . (C.) The proportion of 95% confidence intervals at  $e = [0\%, 20\%]$  that contain the true value of  $w_1$ ,  $w_2$ , and  $w_3$ .

below 70% at  $e = 11\%$  measurement additive error ratio. All three criteria agree that parameter  $w_3$  becomes non-identifiable first as noise increases.

We estimate the parameter  $\beta$  from the modified weak-form input-output equations (13) using WENDy for simulated data with Gaussian additive error. We vary the additive error ratio in the simulated data between  $e = [0\%, 200\%]$  such that the standard deviation of the additive error is  $\sigma = e\text{RMS}(\Omega(t))$ , and at each additive error ratio, we generate 1,000 noisy data sets. The  $(e, q)$ -identifiability for  $e = [0\%, 200\%]$  and  $q = [1\%, 100\%]$  of model (13) is given in Figure 5A. We find that the weak form SIR model is  $(e, q)$ -identifiable for all estimate error ratios above the  $q = 10\%$  level. For measurement error levels from  $[0\%, 120\%]$  the MSE always remains below

$5\% \times \beta$ . Therefore, we conclude the  $\beta$  is generally practically identifiable for noise up to  $120\% \times \text{RMS}(\Omega(t))$ .

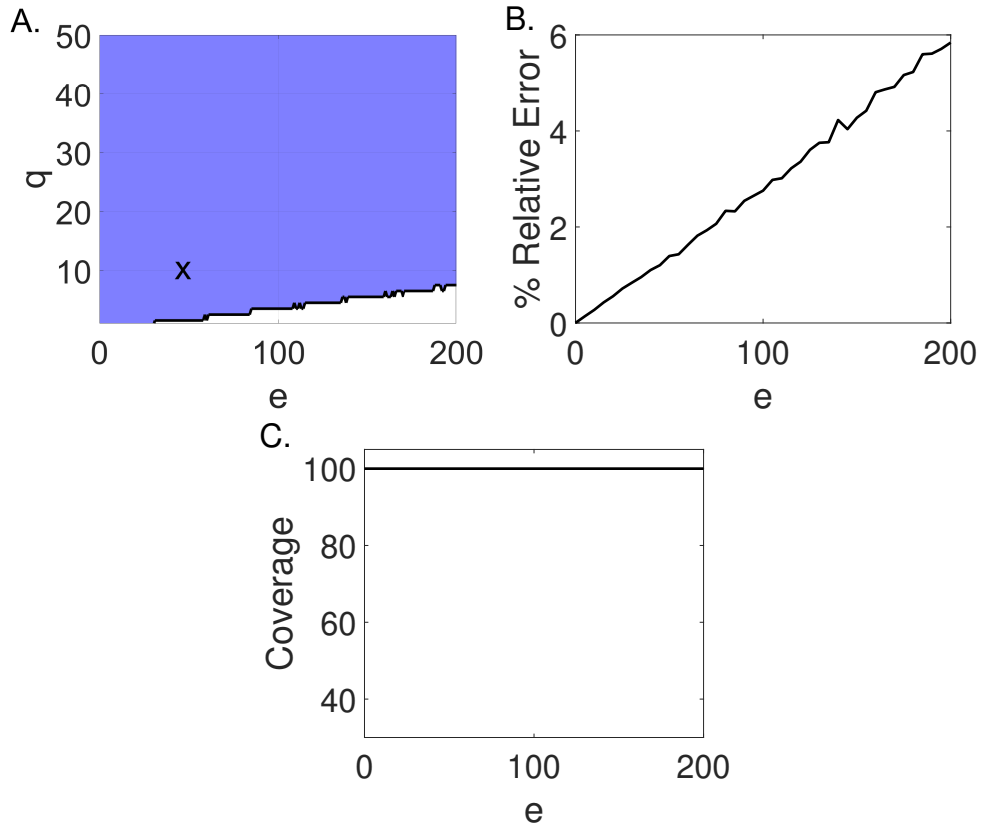


**Fig. 5** Using WENDy with equations (13) we find the SIR model to be generally practically identifiable for additive noise between  $[0\%, 200\%]$ . (A.) The area in blue denotes where the model is (e,q)-identifiable, and the area in white denotes where the model is not (e,q)-identifiable. The (e,q)-identifiability was determined from 1,000 samples at each respective error level, e. The black **X** denotes the (50, 10)-identifiability cutoff. Because this point falls within the blue region, we can say that at a 50% additive error ratio in the data, the MSE of  $\hat{\beta}$  remains below the square of 10% of the magnitude of  $\beta$ . (B.) The relative error determined from 1,000 samples at each respective error level, e. (C.) The proportion of estimated 95% confidence intervals at  $e = [0\%, 200\%]$  that contain the true value of  $\beta$ .

We additionally compare the (e,q)-identifiability of model equations (11)-(12) to the average relative error and the coverage of the 95% confidence intervals generated at each additive error ratio. The relative error generated for 1,000 simulated data sets at each additive error level is given in Figure 5B, and the coverage of the 95% confidence intervals for  $\beta$  is given in Figure 5C. Here, the (e,q)-identifiability and the relative error criteria are in agreement. The relative error remains below 6% even at high additive error ratio,  $e = 200\%$ . Unlike the blood concentration model, the coverage remains 100% across all additive error ratios. However, it is important to note that

while the parameter estimates remain very accurate at high noise, the uncertainty in the estimate still increases with increasing additive noise ( $e$ ) similar to the blood concentration model.

As demonstrated above, often the parameter estimation must be performed many times in order to gain understanding of the practical identifiability of the system, meaning fast estimation methods lead to more convenient assessment of identifiability. Table 1 gives the median time to generate a sample of size  $N = 1,000$  for a 5% additive noise ratio using WENDy on equation (5) and using an output error method on (4). The WENDy method is over twice as fast as the OE method. Additionally, in figure 6, the relative errors in parameter  $w = [w_1, w_2, w_3]$  for 50 simulated data sets of additive error ratios  $e = 0\%, 0.5\%, 1\%, 5\%$ , and  $10\%$  are plotted against the walltime. At all error levels, WENDy is  $5\times$  faster than the output error method. The median walltimes for the WENDy method fall between  $1.27\text{-}2.53\times 10^{-2}$  seconds, while the median output error walltimes fall between  $5.4\text{-}7.3\times 10^{-2}$  seconds. The median relative error is lower for the output error, between  $0.064\text{-}1.7\times 10^{-2}$  for  $e = 0.5\%, 1\%, 5\%, 10\%$  versus between  $0.36\text{-}2.7\times 10^{-2}$  using WENDy. However, the output error is more likely to fail to converge and has a failure rate between  $57.3\%$  and  $63.2\%$ , while the WENDy method converges for all simulated data sets.

Model	WENDy	OE
Blood-tissue diffusion	19 sec	70 sec
SIR	0.7 sec	140 sec

**Table 1** Median time to generate  $N = 1,000$  samples using WENDy method vs OE methods at a 5% additive noise ratio for the Blood-tissue diffusion and SIR models.

In Figure 7, the relative errors in parameter  $\beta$  for 50 simulated data sets of additive error ratios  $e = 0\%, 5\%, 10\%, 15\%$ , and  $20\%$  are plotted against the walltime using WENDy on equations (13) and using an output error method on (9). At all error levels, WENDy is multiple orders of magnitude faster than the output error method. The median walltimes for the WENDy method fall between  $6.4\text{-}9.1\times 10^{-4}$  seconds, while the median output error walltimes fall between  $1.3\text{-}1.6\times 10^{-1}$  seconds. Table 1 shows that the WENDy method can be used in under a second to test practical identifiability on a single error ratio level. The median relative error is similar, within  $2 \times 10^{-3}$ , between the WENDy method and the OE method at error levels  $e = 5\%, 10\%, 15\%$ . However, at the  $e = 20\%$  additive error ratio, the relative error using WENDy is lower,  $4.6 \times 10^{-3}$ , compared to the relative error using the output error,  $1.6 \times 10^{-2}$ . Ultimately, the benefit of smaller walltimes for estimation of parameters in both the blood-tissue diffusion and SIR models allows for the calculations on thousands of simulated data sets, like those used to generate Figures 4 and 5.

## 5 Conclusion

In this work, we present a weak-form framework for efficiently assessing *a priori* model identifiability, summarized below:

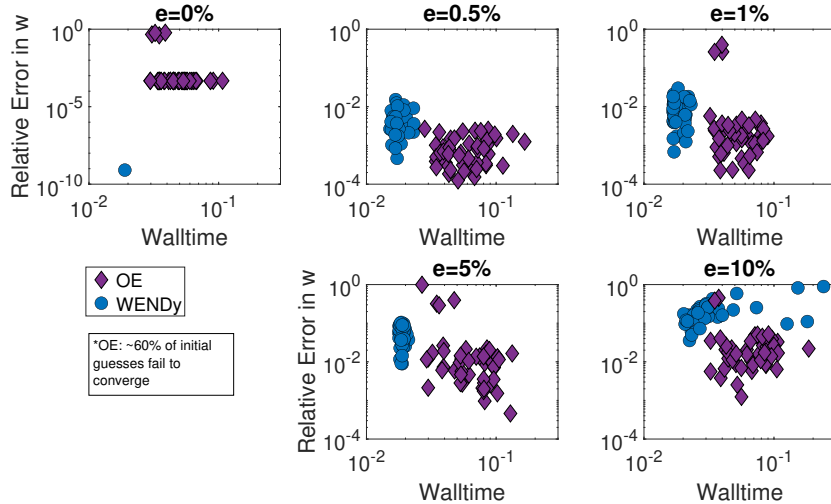


**Fig. 6** Using WENDy with equations (5) we are able to recover the parameters  $w = [w_1, w_2, w_3]$  for the blood-tissue diffusion model from noisy data both more quickly and more consistently than using an output error method. The relative error in  $w$  versus walltime is given for 50 fittings of equations (5) to  $x_1$  compartment data of varying additive error ratios found using WENDy (blue dots) or 50 fittings of model equations (4) using output error (purple diamonds) for additive error ratio between  $e = [0\%, 10\%]$ . Note that for  $\sim 60\%$  of initial guesses fail to converge, and that only successful optimizations for the OE method have been presented above.

1. We apply differential elimination methods to generate an input-output equation. At this step, we can also assess the structural identifiability of the model, which is prerequisite to practical identifiability.
2. We cast the input-output equation into its weak-form. This step involves identifying terms of the weak-form input-output equation where integration by parts can and cannot be applied. Terms where integration by parts is not possible may be managed by either a substitution of variables or an approximation of higher order derivatives.
3. We employ a sampling-based method of assessing practical identifiability. In this process, we generate simulated datasets for various levels of measurement error ratios,  $e$ . We then apply WENDy to weak-form input-output equations for efficient parameter estimation.
4. We assess practical identifiability from these samples using a newly defined criterion,  $(e, q)$ -identifiability.

The  $(e, q)$ -identifiability criterion offers a method for practical identifiability which based on the noise in observed variables  $e$  and the mean-square error of the parameter estimator  $q$ . We demonstrate this  $(e, q)$  criterion via computing the practical identifiability of these two examples in terms of mean-squared error and in terms of average relative error and coverage. This criterion is better able to capture changes in the quality of the parameter estimator due to increased noise in the data compared to criteria

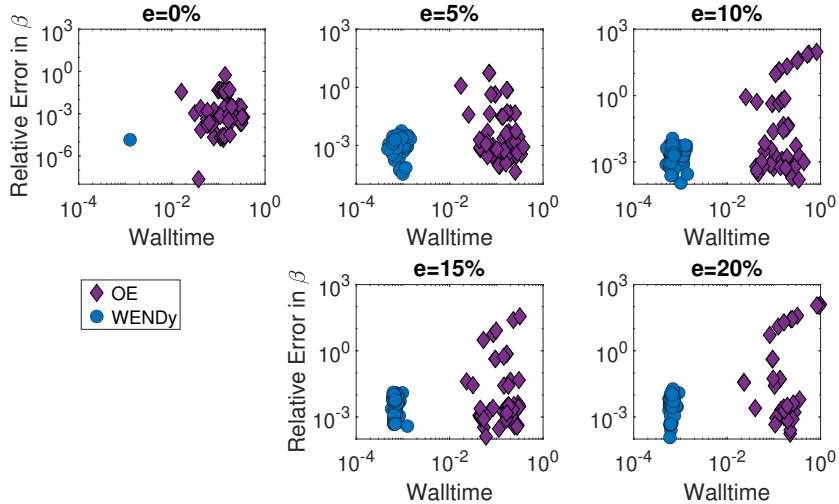


**Fig. 7** Using WENDy with equations (13) we are able to recover the transmission rate  $\beta$  for the SIR model from noisy data, both more quickly than using an output error method. The relative error in  $\beta$  versus walltime is given for 50 fittings of equations (13) to infected compartment data of varying additive error ratio found using WENDy (blue dots) or 50 fittings of model equations (9) using output error (purple diamonds) for additive error ratio between  $e = [0\%, 20\%]$ .

based on average relative errors. Additionally, while in this study we apply the criterion to ODE systems with Gaussian measurement error, it can be extended to a broad range of problems, including discrete-time systems, PDE systems, and problems with non-Gaussian noise, or even multiplicative rather than additive noise.<sup>4</sup> Assessing identifiability in PDE systems is a challenging problem, which has been addressed recently by [46–48], but it still remains difficult (if not impossible) to test structural identifiability for arbitrary PDE systems. Therefore, methods that can efficiently assess the practical identifiability of these systems are particularly important.

Critically, the practical identifiability analyses in this study rely on the efficiency of weak-form parameter estimation. We present a method for weak-form parameter estimation of ODE systems with unobserved compartments, utilizing differential elimination to generate weak-form input-output equations and subsequently applying WENDy. This method is efficient, accurate, and robust to noise. Additionally, applied to a blood-tissue diffusion system (Model (4)), a comparison with the results in [1] yields that the WENDy is better than the Hartley and polynomial test functions and strongly competitive with the interpolated polynomials as well as the pure integral approach.

Regarding method performance, we note that in all the examples presented above (including at all error levels), WENDy is substantially faster than OE methods. In particular, WENDy is faster than the output error method for both the blood-tissue diffusion and SIR models, and is multiple orders of magnitude faster in the SIR case.

<sup>4</sup>Recently, WENDy has been shown to successfully recover parameters from data with multiplicative log-normal noise [45].

Ultimately, the benefit of smaller walltimes for estimation of parameters in both the blood-tissue diffusion and SIR models allows for the calculations on thousands of simulated data sets, like those used to generate Figures 4 and 5. Table 1 demonstrates that for a single error ratio level the WENDy method is able to generate a sample of size  $N = 1,000$  faster than OE methods, with a particularly large advantage (seconds vs minutes) in the SIR model case. For the SIR model the accuracy of the weak-form method is the same as the OE method for additive noise ratios between  $[0\%, 15\%]$ , and more accurate at high noise ratios of  $e = 20\%$ . We further observe that the relative error increases linearly with the additive error ratio for this system. Linear error has also been observed for some systems in [25, 49, 50] when performing EE regression-based optimization. While the median accuracy of the weak-form method is less than the output error method for the blood-tissue diffusion model, the weak-form method does not fail to converge (unlike OE methods, which rely on inspired initial parameter estimates). Notably, for Example 3.1,  $\sim 60\%$  of the OE optimizations failed to converge, even with reasonable initial parameter guesses (see Figure 6).

One limitation of this study is that in the generation of the weak-form input-output equation, information about the initial conditions of the system is lost. There are examples of ODE systems where initial conditions can play an important role in the identifiability of key model parameters [34, 51, 52]. A possible direction to address this limitation is to work with an integral representation of the equation near the end points of the domain to recover information about the initial condition lost in the transformation to the weak form. Future exploration of the impact of initial conditions and methods to incorporate this lost information in our weak-form framework is needed.

Lastly, in this study, we approach practical identifiability through simulated data, and our  $(e, q)$ -criterion provides an *a priori* method of studying model identifiability and robustness to noise. However, it is also of interest to find methods of assessing the identifiability given a specific experimental data set. A future direction of this work could be to explore the relationship between experimental data and the stability of identifiability calculations.

## 6 Acknowledgements

Research reported in this publication was supported in part by the NIGMS Division of Biophysics, Biomedical Technology and Computational Biosciences grant R35GM149335.

## 7 Data and Code Availability

The code for this paper will be provided on Github at <https://github.com/MathBioCU/weak-form-practical-identifiability>.

## References

- [1] Boulier, F., Korporal, A., Lemaire, F., Perruquetti, W., Poteaux, A., Ushirobira, R.: An Algorithm for Converting Nonlinear Differential Equations to

- Integral Equations with an Application to Parameter Estimation from Noisy Data. In: Gerdt, V.P., Koepf, W., Seiler, W.M., Vorozhtsov, E.V. (eds.) *Computer Algebra in Scientific Computing* vol. 8660, pp. 28–43. Springer, Cham (2014). [https://doi.org/10.1007/978-3-319-10515-4\\_3](https://doi.org/10.1007/978-3-319-10515-4_3)
- [2] Nguyen, V.K., Klawonn, F., Mikolajczyk, R., Hernandez-Vargas, E.A.: Analysis of Practical Identifiability of a Viral Infection Model. *PLoS ONE* **11**(12), 0167568 (2016) <https://doi.org/10.1371/journal.pone.0167568>
- [3] Gonçalves, A., Mentré, F., Lemenuel-Diot, A., Guedj, J.: Model Averaging in Viral Dynamic Models. *AAPS J* **22**(2), 48 (2020) <https://doi.org/10.1208/s12248-020-0426-7>
- [4] Stepaniants, G., Hastewell, A.D., Skinner, D.J., Tutz, J.F., Dunkel, J.: Discovering Dynamics and Parameters of Nonlinear Oscillatory and Chaotic Systems from Partial Observations. *arXiv* (2023)
- [5] Simpson, M.J., Maclaren, O.J.: Making Predictions Using Poorly Identified Mathematical Models. *Bull. Math. Biol.* **86**(7), 80 (2024) <https://doi.org/10.1007/s11538-024-01294-0>
- [6] Zitzmann, C., Ke, R., Ribeiro, R.M., Perelson, A.S.: How robust are estimates of key parameters in standard viral dynamic models? *PLoS Comput Biol* **20**(4), 1011437 (2024) <https://doi.org/10.1371/journal.pcbi.1011437>
- [7] Wieland, F.-G., Hauber, A.L., Rosenblatt, M., Tönsing, C., Timmer, J.: On structural and practical identifiability. *Current Opinion in Systems Biology* **25**, 60–69 (2021) <https://doi.org/10.1016/j.coisb.2021.03.005>
- [8] Chis, O., Banga, J.R., Balsa-Canto, E.: Methods for checking structural identifiability of nonlinear biosystems: A critical comparison. *IFAC Proceedings Volumes* **44**(1), 10585–10590 (2011) <https://doi.org/10.3182/20110828-6-IT-1002.00800>
- [9] Miao, H., Wu, H., Xue, H.: Generalized Ordinary Differential Equation Models. *Journal of the American Statistical Association* **109**(508), 1672–1682 (2014) <https://doi.org/10.1080/01621459.2014.957287>
- [10] Stigter, J.D., Molenaar, J.: A fast algorithm to assess local structural identifiability. *Automatica* **58**, 118–124 (2015) <https://doi.org/10.1016/j.automatica.2015.05.004>
- [11] Van Willigenburg, L.G., Stigter, J.D., Molenaar, J.: Sensitivity matrices as keys to local structural system properties of large-scale nonlinear systems. *Nonlinear Dyn* **107**(3), 2599–2618 (2022) <https://doi.org/10.1007/s11071-021-07125-4>
- [12] Villaverde, A.F., Barreiro, A., Papachristodoulou, A.: Structural Identifiability of Dynamic Systems Biology Models. *PLoS Comput Biol* **12**(10), 1005153 (2016)

<https://doi.org/10.1371/journal.pcbi.1005153>

- [13] Ritt, J.: Differential Algebra. Colloquium Publications, vol. 33. American Mathematical Society, Providence, Rhode Island (1950). <https://doi.org/10.1090/coll/033>
- [14] Kolchin, E.R.: Differential Algebraic Groups. Pure and Applied Mathematics, vol. 114. Academic Press, Orlando, FL (1985)
- [15] Ljung, L., Glad, T.: On global identifiability for arbitrary model parametrizations. *Automatica* **30**(2), 265–276 (1994) [https://doi.org/10.1016/0005-1098\(94\)90029-9](https://doi.org/10.1016/0005-1098(94)90029-9)
- [16] Meshkat, N., Eisenberg, M., DiStefano, J.J.: An algorithm for finding globally identifiable parameter combinations of nonlinear ODE models using Gröbner Bases. *Mathematical Biosciences* **222**(2), 61–72 (2009) <https://doi.org/10.1016/j.mbs.2009.08.010>
- [17] Bellu, G., Saccomani, M.P., Audoly, S., D’Angiò, L.: DAISY: A new software tool to test global identifiability of biological and physiological systems. *Computer Methods and Programs in Biomedicine* **88**(1), 52–61 (2007) <https://doi.org/10.1016/j.cmpb.2007.07.002>
- [18] Ciupe, S.M., Tuncer, N.: Identifiability of parameters in mathematical models of SARS-CoV-2 infections in humans. *Sci Rep* **12**(1), 14637 (2022) <https://doi.org/10.1038/s41598-022-18683-x>
- [19] Heitzman-Breen, N., Liyanage, Y.R., Duggal, N., Tuncer, N., Ciupe, S.M.: The effect of model structure and data availability on Usutu virus dynamics at three biological scales. *R. Soc. Open Sci.* **11**(2), 231146 (2024) <https://doi.org/10.1098/rsos.231146>
- [20] Dukic, V., Bortz, D.M.: Uncertainty Quantification Using Probabilistic Numerics: Application to Models in Mathematical Epidemiology. *Inverse Probl. Sci. Eng.* **28**(2), 223–232 (2018) <https://doi.org/10.1080/17415977.2017.1312364>
- [21] Nardini, J.T., Bortz, D.M.: The influence of numerical error on parameter estimation and uncertainty quantification for advective PDE models. *Inverse Problems* **35**(6), 065003 (2019) <https://doi.org/10.1088/1361-6420/ab10bb>
- [22] Shinbrot, M.: On the analysis of linear and nonlinear dynamical systems for transient-response data. Technical Report NACA TN 3288, Ames Aeronautical Laboratory, Moffett Field, CA (December 1954)
- [23] Loeb, J.M., Cahen, G.M.: Extraction a partir des enregistrements de mesures, des parametres dynamiques d’un systeme. *Automatisme* **8**, 479–486 (1963)

- [24] Messenger, D.A., Bortz, D.M.: Weak SINDy For Partial Differential Equations. *J. Comput. Phys.* **443**, 110525 (2021) <https://doi.org/10.1016/j.jcp.2021.110525>
- [25] Messenger, D.A., Bortz, D.M.: Weak SINDy: Galerkin-Based Data-Driven Model Selection. *Multiscale Model. Simul.* **19**(3), 1474–1497 (2021) <https://doi.org/10.1137/20M1343166>
- [26] Bortz, D.M., Messenger, D.A., Dukic, V.: Direct Estimation of Parameters in ODE Models Using WENDy: Weak-form Estimation of Nonlinear Dynamics. *Bull. Math. Biol.* **85**(110) (2023) <https://doi.org/10.1007/S11538-023-01208-6>
- [27] Messenger, D.A., Wheeler, G.E., Liu, X., Bortz, D.M.: Learning anisotropic interaction rules from individual trajectories in a heterogeneous cellular population. *Journal of The Royal Society Interface* **19**(195), 20220412 (2022) <https://doi.org/10.1098/rsif.2022.0412>
- [28] Messenger, D., Dwyer, G., Dukic, V.: Weak-form inference for hybrid dynamical systems in ecology. *Journal of The Royal Society Interface* **21**(221), 20240376 (2024) <https://doi.org/10.1098/rsif.2024.0376>
- [29] Minor, S., Messenger, D.A., Dukic, V., Bortz, D.M.: Learning Weather Models from Data with WSINDy. *arXiv* (2025). <https://doi.org/10.48550/arXiv.2501.00738>
- [30] Denis-Vidal, L., Joly-Blanchard, G., Noiret, C.: System Identifiability (Symbolic Computation) and Parameter Estimation (Numerical Computation). *Numerical Algorithms* **34**(2-4), 283–292 (2003) <https://doi.org/10.1023/B:NUMA.0000005366.05704.88>
- [31] Verdière, N., Denis-Vidal, L., Joly-Blanchard, G., Domurado, D.: Identifiability and estimation of pharmacokinetic parameters for the ligands of the macrophage mannose receptor. *Int. J. Appl. Math. Comput. Sci.* **15**(4), 517–526 (2005)
- [32] Verdière, N., Zhu, S., Denis-Vidal, L.: A distribution input–output polynomial approach for estimating parameters in nonlinear models. Application to a chikungunya model. *Journal of Computational and Applied Mathematics* **331**, 104–118 (2018) <https://doi.org/10.1016/j.cam.2017.09.044>
- [33] Eisenberg, M.C., Robertson, S.L., Tien, J.H.: Identifiability and estimation of multiple transmission pathways in cholera and waterborne disease. *Journal of Theoretical Biology* **324**, 84–102 (2013) <https://doi.org/10.1016/j.jtbi.2012.12.021>
- [34] Chowell, G., Dahal, S., Liyanage, Y.R., Tariq, A., Tuncer, N.: Structural identifiability analysis of epidemic models based on differential equations: A tutorial-based primer. *J. Math. Biol.* **87**(6), 79 (2023) <https://doi.org/10.1007/s00285-023-02007-2>

- [35] Liyanage, Y.R., Heitzman-Breen, N., Tuncer, N., Ciupe, S.M.: Identifiability investigation of within-host models of acute virus infection. *MBE* **21**(10), 7394–7420 (2024) <https://doi.org/10.3934/mbe.2024325>
- [36] Boulier, F.: Differential Elimination and Biological Modelling. In: Rosenkranz, M., Wang, D. (eds.) *Gröbner Bases in Symbolic Analysis*, pp. 109–138. de Gruyter, Berlin, Germany (2007). <https://doi.org/10.1515/9783110922752.109>
- [37] Meshkat, N., Kuo, C.E.-z., DiStefano, J.: On Finding and Using Identifiable Parameter Combinations in Nonlinear Dynamic Systems Biology Models and COMBOS: A Novel Web Implementation. *PLoS ONE* **9**(10), 110261 (2014) <https://doi.org/10.1371/journal.pone.0110261>
- [38] Hong, H., Ovchinnikov, A., Pogudin, G., Yap, C.: SIAN: Software for structural identifiability analysis of ODE models. *Bioinformatics* **35**(16), 2873–2874 (2019) <https://doi.org/10.1093/bioinformatics/bty1069>
- [39] Boulier, F., Thiery, N.: *Differential Algebra V4* (2024)
- [40] Jacquez, J.A., Greif, P.: Numerical parameter identifiability and estimability: Integrating identifiability, estimability, and optimal sampling design. *Mathematical Biosciences* **77**(1-2), 201–227 (1985) [https://doi.org/10.1016/0025-5564\(85\)90098-7](https://doi.org/10.1016/0025-5564(85)90098-7)
- [41] Landaw, E.M., DiStefano, J.J.: Multiexponential, multicompartmental, and non-compartmental modeling. II. Data analysis and statistical considerations. *American Journal of Physiology-Regulatory, Integrative and Comparative Physiology* **246**(5), 665–677 (1984) <https://doi.org/10.1152/ajpregu.1984.246.5.R665>
- [42] Murphy, S.A., Van Der Vaart, A.W.: On Profile Likelihood. *Journal of the American Statistical Association* **95**(450), 449–465 (2000) <https://doi.org/10.1080/01621459.2000.10474219>
- [43] Kreutz, C., Raue, A., Kaschek, D., Timmer, J.: Profile likelihood in systems biology. *The FEBS Journal* **280**(11), 2564–2571 (2013) <https://doi.org/10.1111/febs.12276>
- [44] Tuncer, N., Marctheva, M., LaBarre, B., Payoute, S.: Structural and Practical Identifiability Analysis of Zika Epidemiological Models. *Bull Math Biol* **80**(8), 2209–2241 (2018) <https://doi.org/10.1007/s11538-018-0453-z>
- [45] Rummel, N., Messenger, D.A., Becker, S., Dukic, V., Bortz, D.M.: WENDy for Nonlinear-in-Parameters ODEs. *arXiv* (2025). <https://doi.org/10.48550/arXiv.2502.08881>
- [46] Byrne, H.M., Harrington, H.A., Ovchinnikov, A., Pogudin, G., Rahkooy, H., Soto, P.: Algebraic identifiability of partial differential equation models. *Nonlinearity*

38(2), 025022 (2025) <https://doi.org/10.1088/1361-6544/ada510>

- [47] Ciocanel, M.-V., Ding, L., Mastromatteo, L., Reichheld, S., Cabral, S., Mowry, K., Sandstede, B.: Parameter Identifiability in PDE Models of Fluorescence Recovery After Photobleaching. *Bull Math Biol* **86**(4), 36 (2024) <https://doi.org/10.1007/s11538-024-01266-4>
- [48] Liu, Y., Suh, K., Maini, P.K., Cohen, D.J., Baker, R.E.: Parameter identifiability and model selection for partial differential equation models of cell invasion. *J. R. Soc. Interface* **21**, 20230607 (2024)
- [49] Chen, H.: Data-driven sparse identification of nonlinear dynamical systems using linear multistep methods. *Calcolo* **60**(1), 11 (2023) <https://doi.org/10.1007/s10092-023-00507-7>
- [50] Messenger, D.A., Bortz, D.M.: Asymptotic consistency of the WSINDy algorithm in the limit of continuum data. *IMA Journal of Numerical Analysis*, 086 (2024) <https://doi.org/10.1093/imanum/drae086>
- [51] Miao, H., Xia, X., Perelson, A.S., Wu, H.: On Identifiability of Nonlinear ODE Models and Applications in Viral Dynamics. *SIAM Rev.* **53**(1), 3–39 (2011) <https://doi.org/10.1137/090757009>
- [52] Vasey, G., Messenger, D., Bortz, D., Christlieb, A., O’Shea, B.: Influence of initial conditions on data-driven model identification and information entropy for ideal mhd problems. *Journal of Computational Physics* **524**, 113719 (2025) <https://doi.org/10.1016/j.jcp.2025.113719>

## Appendix A Weak form Estimation of Nonlinear Dynamics (WENDy)

Recently, we have developed the Weak form Estimation of Nonlinear Dynamics (WENDy) method for parameter estimation method [26], which we will briefly describe here. We begin by considering the  $i$ th variable  $u_i$  in a  $d$ -dimensional ordinary differential equation (ODE)

$$\dot{u}_i = \Theta(u)\mathbf{w}_i \tag{A1}$$

with row vector of  $d$  solution states

$$u(t; \mathbf{w}) := (u_1(t; \mathbf{w}), \dots, u_d(t; \mathbf{w}))$$

and row vector of  $J$  features  $\Theta(u) := (f_1(u), \dots, f_J(u))$ . Each feature  $f_j : \mathbb{R}^d \rightarrow \mathbb{R}$  is assumed to be  $C^2$ . We seek to identify the vector of unknown parameters  $\mathbf{w} = [\mathbf{w}_1^T | \dots | \mathbf{w}_d^T]^T \in \mathbb{R}^{Jd}$  from observations of  $u$ .

We let the superscript  $\star$  notation denote quantities based on the true (noise-free and unknown) parameter values ( $\mathbf{w}^\star$ ) and let  $u^\star := u(t; \mathbf{w}^\star)$  and  $\Theta^\star := \Theta(u^\star)$ . We assume that at each timepoint  $t \in \mathbf{t} = (t_0, \dots, t_M)$  measurements of the system are

observed with additive noise

$$U(t) = u^*(t) + \varepsilon(t) \quad (\text{A2})$$

where each element of  $\varepsilon(t)$  is i.i.d.  $\mathcal{N}(0, \sigma^2)$ . Using bold-face variables to represent evaluation at the timegrid  $\mathbf{t}$ , our observations then consist of samples  $\mathbf{U} := \mathbf{u}^* + \boldsymbol{\varepsilon} \in \mathbb{R}^{(M+1) \times d}$ .

To arrive at a weak-form framework to estimate  $\mathbf{w}^*$  from  $\mathbf{U}$ , we consider a  $C^\infty$  bump function  $\phi$  for which the function and all derivatives are compactly supported in the time interval  $[0, T]$  (e.g.  $\phi \in C_c^\infty([0, T])$ ). Multiplying both sides of (A1) by  $\phi$ , and integrating by parts over 0 to  $T$ , we obtain

$$-\int_0^T \dot{\phi} u dt = \int_0^T \phi \Theta(u) \text{mat}(\mathbf{w}) dt, \quad (\text{A3})$$

where “mat” is the matricization operation. Using a set of these test function  $\{\phi_k\}_{k=1}^K$ , (A3) can be discretized at observed data  $\mathbf{U}$ , yielding approximated integrals  $-\Phi_k \mathbf{U} = \Phi_k \Theta(\mathbf{U}) \mathbf{w}$  and corresponding linear system  $\mathbf{G} \mathbf{w}^* \approx \mathbf{b}$ , where

$$\begin{aligned} \mathbf{G} &:= [\mathbb{I}_d \otimes (\Phi \Theta(\mathbf{U}))], \\ \mathbf{b} &:= -\text{vec}(\dot{\Phi} \mathbf{U}). \end{aligned}$$

A simple ordinary least-squares framework for identifying  $\mathbf{w}^*$  does not address the Errors-In-Variables nature of the problem (given the dependence of both  $\mathbf{G}$  and  $\mathbf{b}$  on the noisy data). To address this, the WENDy algorithm uses iterative reweighting to approximate the correct underlying covariance structure. For this purpose, consider the residual

$$\mathbf{r}(\mathbf{U}, \mathbf{w}) := \mathbf{G} \mathbf{w} - \mathbf{b}, \quad (\text{A4})$$

which can be decomposed into several components

$$\mathbf{r}(\mathbf{U}, \mathbf{w}) = \underbrace{(\mathbf{G} - \mathbf{G}^*) \mathbf{w}}_{\mathbf{e}_\Theta} + \underbrace{\mathbf{G}^* (\mathbf{w} - \mathbf{w}^*)}_{\mathbf{r}_0} + \underbrace{(\mathbf{G}^* \mathbf{w}^* - \mathbf{b}^*)}_{\mathbf{e}_{\text{int}}} - \mathbf{b}^\varepsilon. \quad (\text{A5})$$

Here,  $\mathbf{r}_0$  is the residual without measurement noise or integration errors, and  $\mathbf{e}_{\text{int}}$  is the numerical integration error induced by the quadrature. The leftover terms  $\mathbf{e}_\Theta - \mathbf{b}^\varepsilon$  can be Taylor expanded around the data  $\mathbf{U}$ ,

$$\mathbf{e}_\Theta - \mathbf{b}^\varepsilon = \mathbf{L}_\mathbf{w} \text{vec}(\boldsymbol{\varepsilon}) + \mathbf{h}(\mathbf{U}, \mathbf{w}, \boldsymbol{\varepsilon}) \quad (\text{A6})$$

where  $\mathbf{h}(\mathbf{U}, \mathbf{w}, \boldsymbol{\varepsilon})$  denotes higher-order terms in the measurement errors  $\boldsymbol{\varepsilon}$ . The first order matrix in the expansion (A6) is

$$\mathbf{L}_\mathbf{w} := [\text{mat}(\mathbf{w})^T \otimes \Phi] \nabla \Theta \mathbf{K} + [\mathbb{I}_d \otimes \dot{\Phi}],$$

where  $\mathbf{K}$  is the commutation matrix such that  $\mathbf{K}\text{vec}(\boldsymbol{\varepsilon}) = \text{vec}(\boldsymbol{\varepsilon}^T)$ . The matrix  $\nabla\Theta$  contains derivatives of the features (for details see [26]). Under the Gaussian noise assumption, when  $\mathbf{w} = \mathbf{w}^*$  and the integration error is negligible, to first order we have

$$\mathbf{G}\mathbf{w}^* - \mathbf{b} \sim \mathcal{N}(\mathbf{0}, \sigma^2 \mathbf{L}_{\mathbf{w}^*} (\mathbf{L}_{\mathbf{w}^*})^T). \quad (\text{A7})$$

This leads to an iterative algorithm, where the covariance matrix  $\mathbf{C}^{(n)}$  is updated using the weights  $\mathbf{w}^{(n)}$  step  $n$ , for regularization parameter  $\alpha$ ,

$$\begin{aligned} \mathbf{L}^{(n)} &\leftarrow [\text{mat}(\mathbf{w}^{(n)})^T \otimes \Phi] \nabla\Theta(\mathbf{U}) \mathbf{K} + [\mathbb{I}_d \otimes \dot{\Phi}] \\ \mathbf{C}^{(n)} &= (1 - \alpha) \mathbf{L}^{(n)} (\mathbf{L}^{(n)})^T + \alpha \mathbf{I} \end{aligned}$$

and the weights are subsequently updated as

$$\mathbf{w}^{(n+1)} \leftarrow (\mathbf{G}^T (\mathbf{C}^{(n)})^{-1} \mathbf{G})^{-1} \mathbf{G}^T (\mathbf{C}^{(n)})^{-1} \mathbf{b}.$$

## Appendix B Derivations of weak-form input-output equations for SIR model

Consider model equation, which is presented again below,

$$\begin{aligned} \dot{S} &= -\beta SI, \\ \dot{I} &= \beta SI - \alpha I, \\ \dot{R} &= \alpha I. \end{aligned} \quad (\text{B8})$$

By solving for  $S$  from the  $\dot{S}$  equation, we obtain equation the following,

$$S = \frac{\dot{S}}{-\beta I}. \quad (\text{B9})$$

From the  $\dot{S}$  equation we can also obtain equation the following by taking the derivative,

$$\ddot{S} = -\beta \dot{S} I - \beta S \dot{I}. \quad (\text{B10})$$

From the  $\dot{S}$  and  $\dot{I}$  equations we can obtain,

$$\dot{S} = -\beta SI + \alpha I - \alpha I = -(\beta SI - \alpha I) - \alpha I = -\dot{I} - \alpha I. \quad (\text{B11})$$

From the  $\dot{S}$  and  $\dot{I}$  equations we can obtain the following equation by taking the derivative,

$$\ddot{I} = \frac{d}{dt}(\beta SI - \alpha I) = \frac{d}{dt}(-\dot{S} - \alpha I) = -\ddot{S} - \alpha \dot{I}. \quad (\text{B12})$$

Substituting equations (B9) and (B11) in equation (B10) we obtain equation below,

$$\begin{aligned}\ddot{S} &= -\beta\dot{S}I - \beta S\dot{I} = -\beta(-\alpha I - \dot{I})I - \beta\frac{\dot{S}}{-\beta I}\dot{I} \\ &= \beta\alpha I^2 + \beta I\dot{I} + (-\alpha I - \dot{I})\frac{\dot{I}}{I} = \beta\alpha I^2 + \beta I\dot{I} - \alpha\dot{I} - \frac{\dot{I}^2}{I}.\end{aligned}\quad (\text{B13})$$

Next we substitute equation (B13) in equation (B12) to obtain equation (10), an input-output equation for the SIR model for observed state variable  $I$ , which we present again below,

$$\begin{aligned}\ddot{I} &= -\ddot{S} - \alpha I \\ \ddot{I} &= -\beta\alpha I^2 - \beta I\dot{I} + \alpha\dot{I} + \frac{\dot{I}^2}{I} - \alpha\dot{I} \\ 0 &= -\frac{\dot{I}^2}{I} + \beta I\dot{I} + \beta\alpha I^2.\end{aligned}$$

Notice that three of the terms on the right hand side of (10) can be written in the form (1), or in other words can be written a derivative of a function of only  $I$ . However, the term  $\frac{\dot{I}^2}{I}$  cannot be put in this form. We re-write equation (10) in the form (3) by converting as many terms as possible to form (1) to obtain equation the following,

$$0 = -\frac{\dot{I}^2}{I} + \beta\alpha I^2 + \frac{d}{dt}\frac{\beta}{2}I^2 + \frac{d^2}{dt^2}I. \quad (\text{B14})$$

Next, we multiply by test function  $\phi$  and integrate over domain 0 to  $T$  to obtain equation (11), the weak-form SIR input-output equation for observed state  $I$ , which is presented again below,

$$\int_0^T \ddot{\phi} I dt - \int_0^T \phi \frac{\dot{I}^2}{I} dt = \beta \int_0^T \dot{\phi} \frac{I^2}{2} dt - \beta\alpha \int_0^T \phi I^2 dt.$$

From equation (9) we know,

$$\dot{I}^2 = (\beta SI)^2 - 2\beta\alpha SI^2 + \alpha^2 I^2.$$

So, using equation (B11) we can then re-write the term which is not integrable by parts as follows,

$$\frac{\dot{I}^2}{I} = \beta^2 S^2 I - 2\beta\alpha SI + \alpha^2 = \beta S\dot{S} - 2\beta\alpha SI + \alpha^2 I. \quad (\text{B15})$$

Substituting equation (B15) into equation (11) we obtain the following

$$\begin{aligned}\int_0^T \phi \frac{\dot{I}^2}{I} dt &= \beta \int_0^T \phi S \dot{S} dt - \beta \alpha \int_0^T \phi 2SI dt + \alpha^2 \int_0^T \phi dt, \\ &= -\beta \int_0^T \phi \frac{S^2}{2} dt - \beta \alpha \int_0^T \phi 2SI dt + \alpha^2 \int_0^T \phi I dt.\end{aligned}\tag{B16}$$

Let the total population  $N = S(t) + I(t) + R(t)$  be constant. Then,  $S(t) = N - I(t) - R(t)$ . From the equation (9) we know,

$$R(t) = \int_0^t \alpha I(s) ds.$$

Then from our assumption of constant population we are able to generate the following equation from equation (B16), which is given again below,

$$\int_0^T \phi \frac{\dot{I}^2}{I} dt = \beta \int_0^T \phi \frac{(N - R(t) - I)^2}{2} dt - \beta \alpha \int_0^T \phi 2(N - R(t) - I)I dt + \alpha^2 \int_0^T \phi I dt.$$

Finally, we can write equation (13), a weak-form SIR model that reveals parameter  $\beta$  using only observations of state  $I$ , which is given again below,

$$\begin{aligned}\int_0^T \ddot{\phi} I dt - \alpha^2 \int_0^T \phi I dt &= \beta \int_0^T \dot{\phi} \left( \frac{I^2 - (N - R(t) - I)^2}{2} \right) dt \\ &\quad - \beta \alpha \int_0^T \phi (I^2 + 2(N - R(t) - I)I) dt, \\ R(t) &= \int_0^t \alpha I(s) ds.\end{aligned}$$